where Pr is the Prandtl number, θ is the nondimensional temperature, $\theta = T/T_{\text{reference}}$, subscripts s and w correspond to the fluid temperature at the wall and the wall temperature, and $a = (d^2\theta/d\eta^2)_0/(d\theta/d\eta)_0$.

Conclusions

The velocity slip and temperature jump boundary conditions were derived for $Kn \leq 0.5$. Velocity gradient on the wall was obtained from the expansion of the gradient on Knudsen layer unlike the previous analyses that used the expansion of velocity itself. The slip velocities calculated from the present stress boundary condition agreed well with the linearized Boltzmann results.

References

[1]Kennard, E. H., *Kinetic Theory of Gases*, McGraw–Hill, New York, 1938, pp. 295–315.

[2]Arkilic, E. B., Breuer, K. S., and Schmidt, M. A., "Gaseous Flow in Microchannels," *Application of Microfabrication to Fluid Mechanics*, FED Vol. 197, American Society of Mechanical Engineers, Fairfield, NJ, 1994, pp. 57–66.

[3]Harley, J. C., Huang, Y., Bau, H. H., and Zemel. J. N., "Gas Flow in Micro-Channels," *Journal of Fluid Mechanics*, Vol. 284, 1995, pp. 257–274.

[4]Beskok, A., and Karniadakis, G. E., "Models and Scaling Laws for Rarefied Internal Gas Flows Including Separation," 48th Annual Meeting of the American Physical Society Division of Fluid Dynamics, Nov. 1995.

[5]Schaaf, S. A., and Chambre, P. L., *Flow of Rarefied Gases*, Princeton Univ. Press, Princeton, NJ, 1961.

[6]Ohwada, T., Sone, Y., and Aoki, K., "Numerical Analysis of the Poiseuille and Thermal Transpiration Flows Between Two Parallel Plates on the Basis of the Boltzman Equation for Hard-Sphere Molecules," *Physics of Fluids A*, Vol. 1, No. 12, 1989, pp. 2042–2049.

Transient Coupled Radiation and Conduction in a Two-Layer Semitransparent Material

Ping-Yang Wang* and Hui-Er Cheng†
Shanghai Jiaotong University,
200030 Shanghai, People's Republic of China
and
He-Ping Tan‡
Harbin Institute of Technology,
150001 Harbin, People's Republic of China

Introduction

SEMITRANSPARENT material (STM), in which the nature of the radiative transfer can provide a positive or negative internal heat source, is widely applied to engineering. Recently, some researchers have focused on coupled radiation and conduction in a two-layer or multilayer planer STM, such as Ho and Özisik,[1] Spuckler and Siegel,[2] and Siegel.[3] The ray tracing/nodal analysis method was provided in Refs. 4 and 5 to obtain transient temperatures in a single-layer nonscattering STM and isotropically scattering STM, respectively. After that, Refs. 6 and 7 extended this method to a two-layer, isotropically scattering STM with the semitransparent or the opaque boundaries, respectively. Some conclusions were drawn, for example, when one side is heated and the other is cooled, the temperature maximums can appear inside the composite with both semitransparent boundaries[6]; however, for both opaque boundaries the temperature maximums only appear at the heated boundary.[7] The derivation of this method is extended here for a two-layer, isotropically scattering and nongray composite with one semitransparent boundary and one opaque boundary, and the emphasis is placed on investigating whether the peak value of temperature will appear inside the composite and the effects of refractive index and conduction-radiation parameter on temperature distribution. The nomenclature used herein is the same as that of Refs. 6 and 7.

Analysis

A two-layer planar STM with one semitransparent boundary S_1 and one opaque boundary S_2, as shown in Fig. 1, is located between two black surfaces $S_{-\infty}$ and $S_{+\infty}$, which, respectively, denote the outside surroundings. The reflectivities of surfaces S_1, S_P, and S_2 are ρ_1, ρ_P, and ρ_2; the transmissivities of semitransparent surfaces S_1 and S_P are γ_1 and γ_P. The composite is divided into M control volumes. For this physical model the energy equation and the radiative heat source for the transient coupled radiation and conduction are the same as those in Ref. 5, but the radiative transfer coefficient (RTC) and the boundary conditions need to be rededuced. The RTC is defined as the total quotient of the radiative energy arriving at the investigated element in the transfer process and the radiative energy emitted by another one. The transfer process of radiative energy in a scattering STM can be divided into two subprocesses: a nonscattering subprocess and a scattering subprocess.[5] The derivation of scattering subprocess[5] is not provided here because it is independent of the radiative properties of the boundary surfaces. The notation for RTC given in Refs. 6 and 7 is still used, that is, $(S_u S_v)_k$, $(S_u V_j)_k$, and $(V_i V_j)_k$ denote RTCs of surface S_u transferring to surface S_v, surface S_u transferring to volume V_j, and volume V_i transferring to volume V_j for nonscattering materials, respectively; and $[S_u S_v]_k$, $[S_u V_j]_k$, and $[V_i V_j]_k$ denote RTCs for scattering materials. S_u and S_v denote surface $S_{-\infty}$ or S_2; V_i and V_j denote the ith and jth control volumes, respectively; and subscript k refers to the spectral band of interest.

Radiative Transfer Coefficient

Take $(S_{-\infty} V_j)_k$ as an example and assume that V_j belongs to the second layer. The deductive process used in determining the RTCs for diffuse reflection are provided here through tracing the radiative energy by using the philosophy of the ray tracing method in combination with the direct radiative transfer coefficient (DRTC). The DRTC is defined as the RTC not considering reflection and is denoted by $(s_w s_z)_k$, $(s_w v_j)_k$, and $(v_i v_j)_k$, whose equations are given in Ref. 7; s_w and s_z denote surfaces S_1, S_P, or S_2; and v_i and v_j denote control volumes V_i and V_j, respectively.

For the unit radiative energy that comes from $S_{-\infty}$, a part entering the composite through surface S_1 is absorbed by the first layer medium, then transmitted and reflected through surfaces S_1 and S_P. In the end it is attenuated to zero. In this transfer process

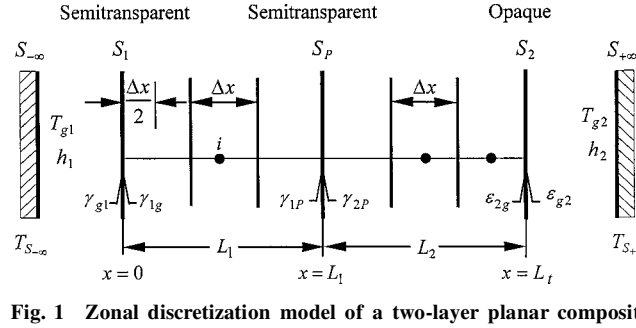

Fig. 1 Zonal discretization model of a two-layer planar composite medium.

Received 25 January 2001; revision received 28 January 2002; accepted for publication 19 March 2002.

*Postdoctor, Institute of Engineering Thermophysics, 1954 Huashan Road.

†Professor, Institute of Engineering Thermophysics, 1954 Huashan Road.

‡Professor, School of Energy Science and Engineering, 92 West Dazhi Street.

the fraction of the total radiative energy reaching surface S_P is $Q_1 = \gamma_1 (s_1 s_P)_k / [1 - \rho_1 \rho_P (s_1 s_P)_k^2]$. Just as with the transfer process in the first layer, Q_1 can be divided into three parts. The first part is absorbed by opaque surface S_2. The second part, denoted by $(S_{-\infty} V_j)_k^{1\text{st}}$, is absorbed by V_j and is called first-order absorption:

$$(S_{-\infty} V_j)_k^{1\text{st}} = Q_1 \gamma_P \frac{(s_P v_j)_k + (s_P s_2)_k \rho_2 (s_2 v_j)_k}{1 - \rho_P \rho_2 (s_2 s_P)_k^2} \tag{1a}$$

The last part comes back to the first layer through interface S_P. During the transfer process in the first layer, part of the energy, denoted by Q_2, enters the second layer. Q_2 can also be divided into three parts just as for Q_1. Thus, the part, denoted by $(S_{-\infty} V_j)_k^{2\text{nd}}$, is absorbed by V_j and is called second-order absorption. For writing convenience, let $FM_{b,k} = \rho_P \rho_b (s_b s_P)_k^2$ ($b = 1$ or 2)[7]; then

$$(S_{-\infty} V_j)_k^{2\text{nd}} = \frac{\gamma_1 \gamma_P (s_1 s_P)_k}{1 - FM_{1,k}} \frac{(s_P v_j)_k + (s_P s_2)_k \rho_2 (s_2 v_j)_k}{1 - FM_{2,k}}$$

$$\times \left[\frac{\gamma_P^2 \rho_1 \rho_2 (s_1 s_P)_k^2 (s_2 s_P)_k^2}{(1 - FM_{1,k})(1 - FM_{2,k})} \right]^1 \tag{1b}$$

By analogy, the $(n+1)$th-order absorption is

$$(S_{-\infty} V_j)_k^{(n+1)\text{th}} = \frac{\gamma_1 \gamma_P (s_1 s_P)_k}{1 - FM_{1,k}} \frac{(s_P v_j)_k + (s_P s_2)_k \rho_2 (s_2 v_j)_k}{1 - FM_{2,k}}$$

$$\times \left[\frac{\gamma_P^2 \rho_1 \rho_2 (s_1 s_P)_k^2 (s_2 s_P)_k^2}{(1 - FM_{1,k})(1 - FM_{2,k})} \right]^n \tag{1c}$$

According to the preceding analysis, in the entire transfer process in which the radiative energy emitted by $S_{-\infty}$ comes into the composite and then is attenuated to zero the total radiative energy absorbed by V_j, that is, radiative transfer coefficient $(S_{-\infty} V_j)_k$, is the sum of the geometric progression represented by Eqs. (1a–1c), that is,

$$(S_{-\infty} V_j)_k = \frac{\gamma_1 \gamma_P (s_1 s_P)_k \left[\left(s_P v_{2_j} \right)_k + (s_P s_2)_k \rho_2 \left(s_2 v_{2_j} \right)_k \right]}{(1 - FM_{1,k})(1 - FM_{2,k})(1 - FM_k)} \tag{1d}$$

The deductive processes for obtaining the other RTCs are not provided because they are similar to $(S_{-\infty} V_j)_k$.

For semitransparent surface S_1 radiative energy can directly transfer from the surroundings to the interior of the composite so that the conduction and convection boundary condition at S_1 is[5]

$$h_1 \left(T_{S_1} - T_{S_{-\infty}} \right) = \frac{2k_1 \left(T_2 - T_{S_1} \right)}{\Delta x}, \qquad x = 0 \tag{2}$$

For opaque surface S_2 there is radiation and conduction between S_2 and the interior of the composite and radiation and convection between S_2 and the surroundings, and so the boundary condition is[5]

$$\sigma \sum_{k=1}^{NB} \left\{ n_{2,k}^2 [S_2 S_{-\infty}]_k A_{k,T_{S_2}} T_{S_2}^4 - [S_{-\infty} S_2]_k A_{k,T_{S_{-\infty}}} T_{S_{-\infty}}^4 \right.$$

$$\left. + \sum_{j=2}^{M+1} \left[n_{2,k}^2 [S_2 V_j]_k A_{k,T_{S_2}} T_{S_2}^4 - n_{j,k}^2 [V_j S_2]_k A_{k,T_j} T_j^4 \right] \right\}$$

$$+ 2k_2 \frac{\left(T_{S_2} - T_{M+1} \right)}{\Delta x} = \sigma \sum_{k=1}^{NB} \varepsilon_2 \left[A_{k,T_{S+\infty}} T_{S+\infty}^4 - A_{k,T_{S_2}} T_{S_2}^4 \right]$$

$$+ h_2 \left(T_{g2} - T_{S_2} \right) \qquad x = 1 \tag{3}$$

Let $b = 1$ or 2. In the preceding equations h_b is the convective heat-transfer coefficient at surface S_b, $\mathrm{Wm^{-2}K^{-1}}$; T_{S_b} is the temperature of surface S_b, K; T_{gb} is the gas temperature for convection at S_b, K; k_b is the conductivity of the bth layer, $\mathrm{Wm^{-1}k^{-1}}$; Δx is the spatial interval, m; σ is the Stefan–Boltzmann constant, $\mathrm{Wm^{-2}K^{-4}}$; NB is the total number of spectral bands; n_j is the refractive index; ε_2 is the emissivity of surface S_2; and

$$A_{k,T_i} = \int_{\Delta\lambda_k} \frac{I_{b,\lambda}(T_i)\, \mathrm{d}\lambda}{n_i^2 \sigma T_i^4}$$

is the fractional spectral emissive power of spectral band k at nodal temperature T_i.

The reflectivity of the semitransparent surface is obtained by Fresnel's relation,[7] and for other details about the ray tracing/nodal analysis method, refer to Refs. 4–7.

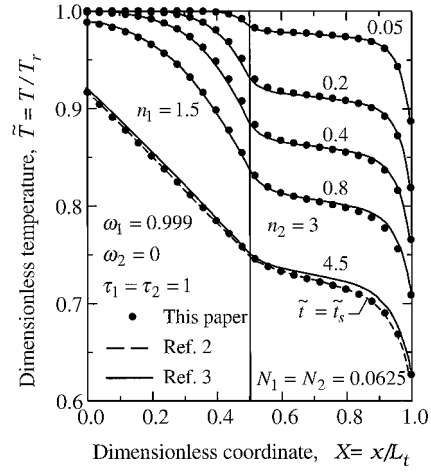

Fig. 2 Comparison of present results with those of Refs. 2 and 3.

Verification

For the ray tracing/nodal analysis method Refs. 6 and 7 have provided a number of comparisons with previous results. This method is extended here to two-layer composites with one semitransparent and one opaque boundary. No research on this subject has been found. Therefore, to partially validate the present solution Fig. 2 provides a comparison with an exact numerical solution[2] and an approximate solution using the Green's function and the two-flux method[3] for a two-layer and gray STM with both semitransparent boundaries. The input parameters were taken as dimensionless surroundings temperature for radiation $\tilde{T}_{S_{-\infty}} = T_{S_{-\infty}}/T_r = 1$, $\tilde{T}_{S_{+\infty}} = 0.25$; T_r is the reference temperature and the uniform initial temperature; dimensionless gas temperatures for convection $\tilde{T}_{g1} = 1$, $\tilde{T}_{g2} = 0.25$; and convection-radiation parameter $H_b = h_b/4\sigma T_r^3 = 0.25$. In Fig. 2 $\tilde{t} = (4\sigma T_r^3/C_1 L_t)t$ is dimensionless time; t is the physical time, s; C_1 is the specific heat capacity of the first layer, $\mathrm{J\,kg^{-1}\,K^{-1}}$; L_t is the total thickness, m; $\tilde{t}_s$ denotes the steady-state dimensionless time; τ_b is the optical thickness; ω_b is the single-scattering albedo; and N_b is the conduction-radiation parameter and $N_b = k_b/(4\sigma T_r^3 L_t)$. As shown in Fig. 2, the present results are almost the same as the exact numerical solution so that it is difficult to distinguish, whereas the approximate results in Ref. 3 deviate only a little from the results in Ref. 2. This demonstrates that the present method is more accurate because the space solid angle is not dispersed.

Results

For convenience, all of the following results are for the gray composite, that is, $NB = 1$, although the equations of this Note have considered the spectral properties by using spectral bands.

Effect of Radiative Boundary Condition

To investigate whether the peak value of temperature appears inside the composite, both combinations of the radiative boundary condition are chosen: 1) semitransparent surface S_1 is heated by radiation from the environment and opaque surface S_2 is cooled, that is, $\tilde{T}_{S_{-\infty}} = 1.5$ and $\tilde{T}_{S_{+\infty}} = 0.5$; 2) and the reverse of condition 1), that is, $\tilde{T}_{S_{-\infty}} = 0.5$ and $\tilde{T}_{S_{+\infty}} = 1.5$. Figure 3 illustrates the transient

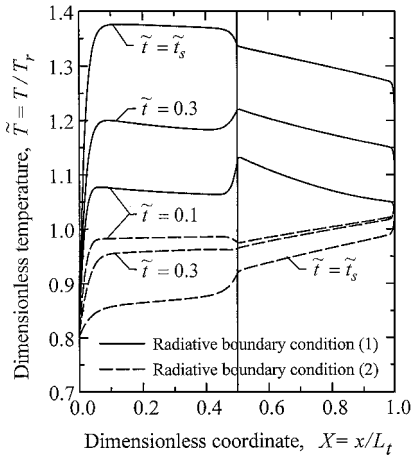

Fig. 3 Transient temperature distribution for both combinations of the radiative boundary condition.

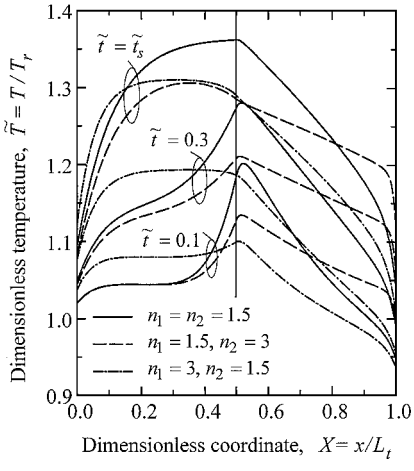

Fig. 4 Effect of refractive index on temperature distribution.

temperature distribution in the two-layer gray composite with diffuse surfaces. Other parameters are chosen as $H_1 = H_2 = 1.25$, $\tilde{T}_{g1} = 0.8$, $\tilde{T}_{g2} = 1.0$, $n_1 = 1.5$, $n_2 = 3$, $\varepsilon_2 = 0.2$, $\tau_1 = 0.1$, $\tau_2 = 5$, $\omega_1 = 0$, $\omega_2 = 0.5$, and $N_1 = N_2 = 0.0025$. Under the conditions of this Note, when the boundary surface heated by radiation is semitransparent the maximum temperature appears in the composite throughout the transient and steady state because the radiative energy of the surroundings can be directly transferred to the interior of the composite. Even two peak values of temperature are formed for small $\tilde{t}$. For radiative boundary condition 2 the temperature distributions are very different from those for radiative boundary condition 1, and the maximum temperature can only appear at the opaque surface heated by outer radiation because the radiative energy can only transfer to the interior of the STM from the heated boundary surfaces by radiation and conduction. However, the peak value of transient temperature may appear inside the composite for radiative boundary condition 2 because S_1 is semitransparent.

Effect of Refractive Index

Figure 4 illustrates the effect of the refractive index on the transient temperature distribution in the two-layer gray composite with diffuse surfaces. Boundary S_1 is semitransparent, and S_2 is opaque. Three combinations of the refractive index are chosen: a) $n_1 = n_2 = 1.5$; b) $n_1 = 1.5$, $n_2 = 3$; and c) $n_1 = 3$, $n_2 = 1.5$. Other parameters are taken as $\tilde{T}_{S-\infty} = 1.5$, $\tilde{T}_{S+\infty} = 0.5$, $H_1 = H_2 = 1.25$, $\tilde{T}_{g1} = \tilde{T}_{g2} = 1$, $\tau_1 = 0.1$, $\tau_2 = 5$, $\omega_1 = \omega_2 = 0$, and $N_1 = N_2 = 0.05$. For convenience of comparison, the emissivity of the opaque surface is obtained from the reflectivity of the surface without coating. As shown in Fig. 4, increasing the refractive index, whether the first layer or the second layer, provides decreased average temperature

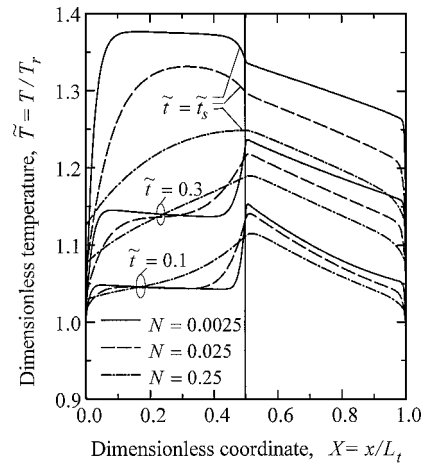

Fig. 5 Effect of conduction-radiation parameter on temperature distribution.

and maximum temperature, and the temperature distribution is more uniform in the layer with the larger refractive index. When $n_1 = 3$, $n_2 = 1.5$, larger reflectivities ρ_{g1} and ρ_{1P} prevent radiative energy from coming into the second layer and the temperature in that layer decreases.

Effect of Conduction-Radiation Parameter

The effects of conduction-radiation parameter $N = N_1 = N_2$ on temperature distribution are shown in Fig. 5. Chosen conduction-radiation parameter include $N = 0.0025$ (solid line), 0.025 (dash line), and 0.25 (dot–dash line). Refractive index $n_1 = 1.5$ and $n_2 = 3.0$. The other parameters are the same as Fig. 4. As shown in Fig. 5, with increasing of N the effect of conduction strengthens, so for a heated semitransparent boundary surface the maximum steady-state temperature moves to the interior of the composite, but the location of the maximum transient temperature is almost changeless because radiant propagation is more rapid than conduction. The effect of N on the temperature distribution is also correlative to the optical thickness. Because the first layer is optically thin ($\tau_1 = 0.1$) and the second layer is optically thick ($\tau_2 = 5$), the effect of N on the temperature distribution in the first layer is larger than that in the second layer.

Conclusions

By analyzing the present results, the following conclusions are drawn: When the semitransparent boundary is radiatively heated and the opaque boundary is radiatively cooled, the steady-state and transient temperature maximums may appear inside the composite. In addition, two temperature peaks are likely to appear inside the composite for the small dimensionless time. When the radiative boundary conditions are reversed, the maximum temperature only appears at the heated surface. However, the transient temperature peak value may also appear inside the composite. An inhomogeneous STM can be equivalent to a composite composed of the multilayer STM with different thermophysics properties. Therefore, we can predict that one or more peak values of the transient and steady-state temperature may still appear inside the inhomogeneous STM when the boundary subjected to high-temperature radiative surroundings is semitransparent and the other boundary, whether it is semitransparent or opaque, is subjected to low-temperature surroundings.

Acknowledgments

This research is supported by the Chinese National Science Fund for Distinguished Young Scholars (No. 59725617), National Natural Science Foundation of China (No. 59806003).

References

[1] Ho, C. H., and Özisik, M. N., "Simultaneous Conduction and Radiation in a Two-Layer Planar Medium," *Journal of Thermophysics and Heat Transfer*, Vol. 1, No. 2, 1987, pp. 154–161.

[2]Spuckler, C. M., and Siegel, R., "Refractive Index and Scattering Effects on Radiation in a Semitransparent Laminated Layer," *Journal of Thermophysics and Heat Transfer*, Vol. 8, No. 2, 1994, pp. 193–201.

[3]Siegel, R., "Green's Function and Two-Flux Analysis for Transient Radiative Transfer in a Composite Layer," *Proceedings of the National Heat Transfer Conference*, HTD Vol. 325, edited by A. M. Smith, American Society of Mechanical Engineers, New York, 1996, pp. 35–43.

[4]Tan, H. P., and Lallemand, M., "Transient Radiative—Conductive Heat Transfer in Flat Glasses Submitted to Temperature, Flux and Mixed Boundary Conditions," *International Journal of Heat and Mass Transfer*, Vol. 32, No. 5, 1989, pp. 795–810.

[5]Tan, H. P., Ruan, L. M., Xia, X. L., Yu, Q. Z., and Tong, T. W., "Transient Coupled Radiative and Conductive Heat Transfer in an Absorbing, Emitting, and Scattering Medium," *International Journal of Heat and Mass Transfer*, Vol. 42, No. 15, 1999, pp. 2967–2980.

[6]Tan, H. P., Wang, P. Y., and Xia, X. L., "Transient Coupled Radiation and Conduction in an Absorbing and Scattering Composite Layer," *Journal of Thermophysics and Heat Transfer*, Vol. 14, No. 1, 2000, pp. 77–87.

[7]Wang, P. Y., Tan, H. P., Liu, L. H., and Tong, T. W., "Coupled Radiation and Conduction in a Scattering Composite Layer with Coatings," *Journal of Thermophysics and Heat Transfer*, Vol. 14, No. 4, 2000, pp. 512–522.

Axial Thermal Dispersion Conductivity of Open-Cellular Porous Materials

Kouichi Kamiuto* and San San Yee†
Oita University, Oita 870-1192, Japan

Nomenclature

c_{pf} = specific heat of fluid at constant pressure, J/kg K
D_n = nominal cell diameter, 0.0254/pores per inch, m
G = incident radiation, W/m^2
$\tilde{g}^*$ = asymmetry factor of the scattering phase function
k = permeability, m^2
k_{da} = axial thermal dispersion conductivity, W/mK
k_{ec} = effective conductive thermal conductivity, W/mK
k_f = thermal conductivity of gas, W/mK
k_t = total effective thermal conductivity, $k_{ec} + k_{da}$, W/mK
Nl = volume of gas at 273.15 K and 1.0133 bar
Pr = Prandtl number
q_{RS} = irradiation on the upper surface of a porous cylinder, W/m^2
Re = Reynolds number defined by $u_m \rho_f \sqrt{k}/\mu_f$
T = temperature, K
T_R = equivalent blackbody temperature, K
T_s = mean temperature of the upper surface of a porous cylinder, K
T_0 = inlet air temperature, K
u_m = mean gas velocity, m/s
w = dimensionless width of a strut with a square cross section, $\frac{1}{2} + \cos[(\frac{1}{3})\cos^{-1}(2\phi - 1) + 4\pi/3]$
z = axial coordinate, m
z_0 = length of a porous cylinder, m
β^* = scaled extinction coefficient, m^{-1}
γ_a = axial thermal dispersion coefficient for open-cell foams
γ_a^* = axial thermal dispersion coefficient for packed-sphere systems
γ_r = radial thermal dispersion coefficient for open-cell foams
γ_r^* = radial thermal dispersion coefficient for packed-sphere systems
μ_f = viscosity, Pa · s
π = ratio of the circumference to its diameter of a circle
ρ_f = density of fluid, kg/m^3
ρ_H = hemispherical reflectivity of the surface of skeletons consisting of an open-cell foam
σ = Stefan–Boltzmann's constant, W/(m^{2}K^4)
ϕ = porosity
ω^* = scaled albedo

Received 4 February 2002; revision received 25 March 2002; accepted for publication 25 March 2002.

*Professor, Department of Production Systems Engineering, Dannoharu 700; kamiuto@cc.oita-u.ac.jp. Senior Member AIAA.

†Graduate Student, Graduate School, Dannoharu 700.

Introduction

OPEN-CELLULAR porous materials consisting of pentagonal dodecahedron cells with open-cell walls have been widely utilized as elements of radiators, catalytic converters, regenerative heat exchangers, combustors, and so forth.[1,2] With regard to thermal design and operation of these facilities, fundamental knowledge of the heat transfer characteristics of this kind of porous medium has been needed.[3] A few sets of heat transfer parameters are required in accord with the heat transfer model adopted: When local thermal equilibrium between fluid and solid phases exists within a medium and, hence, the one-temperature model is acceptable as a heat transfer model, only the effective conductive thermal conductivity k_{ec} and axial thermal dispersion conductivity k_{da} are necessary, whereas if the local thermal equilibrium assumption could not be justified and, thus, the two-temperature model must be utilized, the volumetric heat transfer coefficient h_v is also required in addition to the aforementioned parameters. In any case, both k_{ec} and k_{da} are indispensable to heat transfer models of an open-cellular porous medium.

A number of experimental and theoretical studies of k_{ec} have been made during recent decades, and, at present, there exists an accurate theoretical model to predict k_{ec} such as Schuetz–Glicksman's model,[4] but there has been no effort to determine the effective thermal conductivity in the axial direction.[2]

The purpose of the present Note is to remedy this deficiency. To this end, the axial thermal dispersion conductivities of open-cellular condierite–alumina porous materials are determined by an inverse analysis of steady-state axial temperature profiles of the open-cell foams, where radiant energy from infrared lamps flowed countercurrently to the flow of fluid.

Experimental Apparatus and Procedures

The test section for measuring the axial temperature distributions within a porous medium to estimate the axial total effective thermal conductivity consists of a circular steel pipe 0.11 m in inner diameter and 0.17 m in height, where an open-cellular cordierite–alumina porous cylinder 0.1 m in diameter and 0.15 m in height was concentrically placed. A gap between the porous cylinder and the inner wall of the test pipe was filled with clay. The outer surface of the steel pipe was insulated by 0.05-m-thick fiber insulation.

Nine type-K sheathed thermocouples of 0.0016-m diam were inserted through the pipe wall along the central axis of the cylinder to provide information on the axial temperature distribution. In addition, four type-K sheathed thermocouples were settled along the off-central axis, being 0.025 m apart from the central axis, to check radial temperature uniformity within the porous cylinder. Several type-T thermocouple elements were adhered on the upper and lower surfaces of the cylinder (five for the upper surface and two for the lower surface). Inlet air temperature was also measured by type-K sheathed thermocouples.

Four 250-W infrared lamps were used to heat the upper surface of the porous cylinder radiatively and to form an axial temperature gradient within the porous medium. The amount of radiant energy from the infrared lamps was measured on the upper surface of the porous cylinder using a still-type water calorimeter that consists of a 0.1-m-inner diameter and 0.0015-m-thick Bakelite disk with 0.003-m-highrim and 1.3×10^{-5} m thick polyethylene film and that contains 0.025 kg of water. The relative uncertainity in measuring the irradiation was estimated to be ±4%.